The Sensitivity of Meta Distributions to Their Moments

Xinyun Wang, *Graduate Student Member, IEEE*, and Martin Haenggi, *Fellow, IEEE*

***Abstract*—While meta distribution (MD) reconstruction methods based on moments play an important role in analyzing wireless network performance, a critical gap exists in comprehending the impact and consequences of inaccurate moments on MD reconstructions. The reliability and robustness of these techniques remain unexplored. In this paper, we address this gap by analyzing the sensitivity of commonly used MD reconstruction methods to perturbations to moments and provide valuable guidelines for the application of these methods. Furthermore, we quantify the impact of inaccurate moments on MD reconstructions, examining the validity of perturbed moment sequences and demonstrating the critical importance of moment accuracy. Our investigation demonstrates the necessity for precise moment computation. Succinctly put, moment quality is preferred over moment quantity.**

***Index Terms*—Sensitivity, meta distribution, Hausdorff moment problem, stochastic geometry**

I. INTRODUCTION

A. Meta distributions and the truncated Hausdorff moment problem

With the rapid proliferation of smart devices, there is an increasing demand for wireless networks to support sophisticated applications like augmented reality and interactive online gaming. Users expect consistent performance and reliability. However, despite manufacturers and service providers often highlighting peak performance in their advertisements, the actual user experience differs from both peak and average performance. Instead, it is crucial to consider the performance achievable by different percentiles of users, such as the 95-th, 50-th, or 5-th percentile. Recent evaluations of wireless network performance, including those for 5G and WiFi standards [1], [2], have focused on specifying the throughput levels that 95% of users should achieve. Theoretical approaches often only analyze the distribution of the signal-to-interference ratio (SIR), from which the data rate or the spectral efficiency can be derived. This kind of distribution averages over all sources of randomness, such as point process(es), fading, shadowing, and channel access schemes, making it impossible to separate the impact of individual random elements. As a result, it fails to capture the performance at the individual link level. The meta distribution (MD) of the SIR resolves this problem by separating different sources of randomness via conditional probabilities [3]–[7]. Typically an SIR MD is defined as the complementary cumulative distribution function (cdf) of the conditional probability

$$P_t \triangleq \mathbb{P}(\mathrm{SIR} > t \mid \Phi), \quad t \in \mathbb{R}^+,$$

where Φ is the point process, i.e., the SIR MD is given by

$$\bar{F}(x,t) \triangleq \mathbb{P}(P_t > x), \quad x \in [0,1], t \in \mathbb{R}^+.$$

While it allows for a much sharper performance characterization, it can in most cases only be calculated based on the moments of the underlying conditional distribution [3]–[9]. The z-th moment of P_t is

$$m_z(t) \triangleq \int_0^1 z x^{z-1} \bar{F}(x,t)\, dx, \quad z \in \mathbb{C}. \tag{1}$$

The problem of recovering a distribution from a limited number of its moments is formulated as follows: given a finite-length sequence $(m_k)_{k=1}^n$, $n \in \mathbb{N}$, find or approximate an F that solves

$$\int_0^1 x^k \, dF(x) = m_k, \quad k = 0, 1, ..., n, \tag{2}$$

where F is right-continuous and increasing with $F(0^-) = 0$ and $F(1) = 1$, i.e., F is the cumulative distribution function (cdf) of a random variable supported on $[0,1]$. $m_0 = 1$ is assumed fixed. Let $\mathcal{F}_n$ denote the family of F whose first n moments match $(m_k)_{k=1}^n$. This problem is called the *truncated Hausdorff moment problem* [10]. In most cases, when a solution exist to the truncated Hausdorff moment problem, it is one of infinitely many [10], [11].

The truncated Hausdorff moment problem, i.e., using moments to reconstruct the distributions, has been an important topic in the analysis of MDs [3], [8], [9], [12]. A key issue that has not been considered is that the numerically obtained values of the moments deviate from the exact ones, i.e., they are *perturbed*. The causes for the perturbations are the use of simplified models to approximate the actual moments (see, e.g., [7]) and inaccurate evaluations of exact but complicated expressions (see, e.g., [13]). The implications can be divided into two categories: (1) The perturbations can invalidate the moment sequences, i.e., turn them into sequences that cannot be the moments of a distribution; (2) they can change the solutions or approximations to the truncated Hausdorff moment problem.

While perturbations affect the solutions/approximations to the truncated Hausdorff moment problem in general, our focus is on MDs that arise in wireless networks, specifically the SIR MDs.

The authors are with the Department of Electrical Engineering, University of Notre Dame, Notre Dame, IN 46556, USA. (e-mail: {xwang54, mhaenggi}@nd.edu).

This work was supported in part by the U.S. National Science Foundation (grant CCF 2007498).

B. A motivating example: the Chebyshev-Markov (CM) inequalities of order 2

Here we focus on the well-known Chebyshev-Markov (CM) inequalities. These inequalities offer the tightest possible bounds on the distributions whose first n moments match a given sequence of length n [10], [14]. These bounds are achieved by certain discrete distributions whose moments match the given sequence. We aim to investigate how perturbations in the moments change the tightest possible bounds. Specifically, we would like to explore how the infima and suprema of all possible solutions to the matching moment sequence change when there is a small variation in the second moment. We set $n = 2$ for ease of exposition.

Example 1 ($n = 2$)**.** *For $n = 2$, consider the case with positive variance, i.e., $m_2 > m_1^2$. Let h denote $\frac{m_1 - m_2}{1 - m_1}$. It is obvious that $h < \frac{m_2}{m_1}$. The infima and suprema are*

$$\inf_{F \in \mathcal{F}_2} F(x) = \begin{cases} 0, & 0 \le x \le h, \\ 1 - \frac{m_1 - m_2}{x} - m_1, & h < x \le \frac{m_2}{m_1}, \\ \frac{(x - m_1)^2}{m_2 - m_1^2 + (x - m_1)^2}, & \frac{m_2}{m_1} < x \le 1, \end{cases} \tag{3}$$

$$\sup_{F \in \mathcal{F}_2} F(x) = \begin{cases} \frac{m_2 - m_1^2}{m_2 - m_1^2 + (x - m_1)^2}, & 0 \le x \le h, \\ 1 + \frac{m_1 - m_2}{1 - x} - m_1, & h < x \le \frac{m_2}{m_1}, \\ 1, & \frac{m_2}{m_1} < x \le 1. \end{cases} \tag{4}$$

Consider two sequences $\mathbf{m} = (1, m_1, m_2)$ and $\mathbf{m}' = (1, m_1, m_2')$ where $m_1 \in (0, 1)$ and $m_2, m_2' \in (m_1^2, m_1)$. These conditions ensure that $\mathbf{m}$ and $\mathbf{m}'$ are two valid moment sequences. Let $\mathcal{F}_2$ and $\mathcal{F}_2'$ denote the families of cumulative distribution functions (cdfs) whose first two moments match $\mathbf{m}$ and $\mathbf{m}'$, respectively. Assume $\Delta m_2 = m_2' - m_2 > 0$ so that $\frac{m_1 - m_2}{1 - m_1} > \frac{m_1 - m_2'}{1 - m_1}$ and $\frac{m_2}{m_1} < \frac{m_2'}{m_1}$. For $x \in [\frac{m_1 - m_2}{1 - m_1}, \frac{m_2}{m_1}]$,

$$\inf_{F \in \mathcal{F}_2'} F(x) - \inf_{F \in \mathcal{F}_2} F(x) = \Delta m_2 / x \tag{5}$$

and

$$\sup_{F \in \mathcal{F}_2'} F(x) - \sup_{F \in \mathcal{F}_2} F(x) = -\Delta m_2 / (1 - x). \tag{6}$$

Therefore, on the interval $[\frac{m_1 - m_2}{1 - m_1}, \frac{m_2}{m_1}]$, the difference in the lower bounds and that in the upper bounds exhibit an odd symmetry with respect to (wrt) the point $(0.5, 0)$. Because of the symmetry, in the following, we focus on the lower bounds only. Notably, the disparity in the tightest lower bounds on the interval $[\frac{m_1 - m_2}{1 - m_1}, \frac{m_2}{m_1}]$ is directly proportional to the difference in m_2 and inversely proportional to x. Consequently, as x approaches 0, minor perturbations in m_2 can lead to substantial differences, potentially magnifying the lower bounds tenfold or even hundredfold. Also, on the interval $[\frac{m_1 - m_2'}{1 - m_1}, \frac{m_1 - m_2}{1 - m_1}]$, the difference increases as x increases, due to the fact that one of the lower bounds stays zero. Therefore, the maximum difference is achieved at $x = \frac{m_1 - m_2}{1 - m_1}$.

Figure 1 shows an example of $m_1 = 0.5, m_2 = 0.4894$ and $m_2' = 0.4954$. The difference in m_2 is just 0.006 (corresponding to a perturbation of 1.23%) while the difference in the infima around $x = 0.02$ is 50 times bigger. This shows that inaccuracies in the calculations of the moments can have a drastic impact on the reconstructed MD.

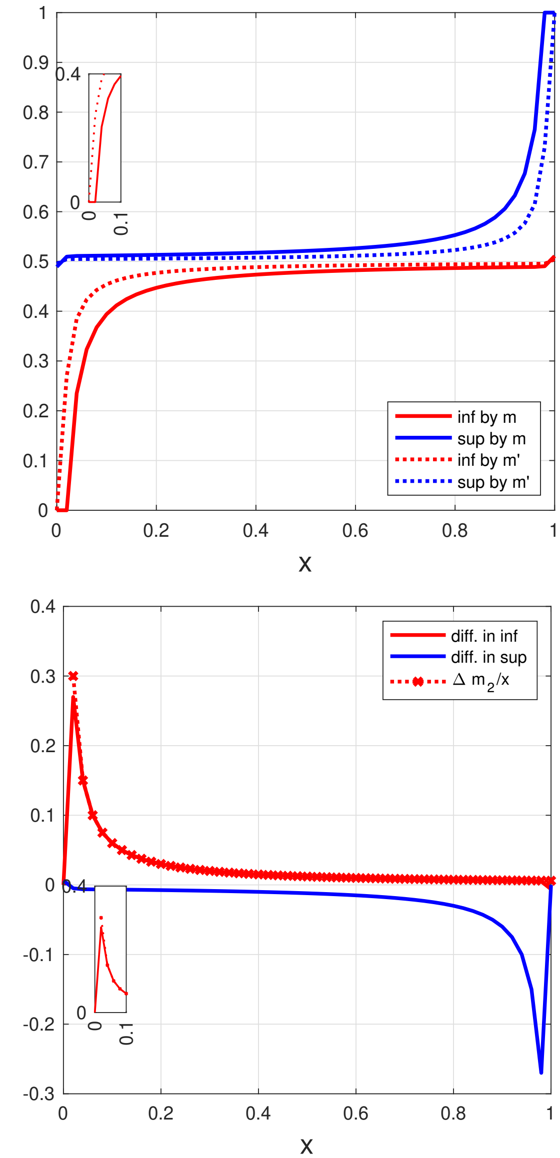

Fig. 1. The top plot shows the tightest possible bounds by the CM inequalities for $\mathbf{m} = (1, 0.5, m_2 = 0.4894)$ and $\mathbf{m}' = (1, 0.5, m_2 = 0.4954)$, respectively. The bottom plot shows the difference in the bounds for $\mathbf{m}$ and $\mathbf{m}'$.

C. Related works and contributions

While MD reconstruction methods and their applications have garnered considerable attention [3], [8], [9], [12], the implications of inaccurate moments on MD reconstructions have not been explored, leaving unanswered questions about the reliability and robustness of MD reconstruction methods. Our work fills this gap. Our contributions are summarized as follows.

- Sensitivity analysis: We conduct a thorough analysis of the sensitivity of commonly used MD reconstruction methods and provide comprehensive guidelines for their applications. Studying the sensitivity of these methods to variations in the moments provides important insights to researchers, facilitating more informed decision-making in their choice and implementation of MD reconstruction techniques.

- Robustness metric: We introduce a single-letter robustness metric that quantifies how susceptible a moment sequence is to perturbations. With this metric, we can assess the necessity for higher accuracy settings.
- Effect of inaccurate moments: We discuss the impact of inaccurate moments on MD reconstructions. We investigate the validity of perturbed moment sequences and examine their impact on the corresponding MDs and show the importance of the accuracy of moments.
- Guidance for limited computational resources: We give comprehensive guidance for effectively calculating and utilizing moments in MD reconstructions. Our guidelines offer practical strategies for optimizing computational resources while ensuring robust and reliable MD reconstructions. By addressing the challenges associated with resource constraints, we help researchers make efficient use of available resources in the MD reconstruction process.

Notation. $[n] \triangleq \{1, 2, ..., n\}$ and $[n]_0 \triangleq \{0\} \cup [n]$. $\mathbb{N}$ is the set of positive integers. $\mathbb{N}_0$ is the set of non-negative integers. $\mathbb{R}^+$ is the set of positive real numbers. $\mathbb{C}$ is the set of complex numbers.

II. Source of perturbations

Perturbations to moments arise from two sources: the use of approximated moment expressions (see, e.g., [7]), and the inaccurate numerical evaluations of complicated exact moment expressions (see, e.g., [13]). Given the inherent uncertainty of the accuracy of approximated moment expressions, our discussion focuses on the scenarios where moment expressions are precisely known. Inaccurate evaluations of precisely known moment expressions often arise from the numerical integration of complicated integral expressions, such as double and triple integrals, in particular if the domain of integration is unbounded. In this section, we first discuss some common numerical integration techniques (when the domains of integration are finite and the integrands are bounded) for proper integrals and the corresponding errors, then we explore the error in a wireless network example, and lastly we examine the errors resulting from truncation for improper integrals (when the domain of integration is unbounded and the integrands are bounded).

A. Numerical integration methods

Due to the complicated nature of some of the moment expressions, numerical integration is necessary to approximate the integrals through discrete methods. The accuracy of numerical integration can be compromised by various factors. In this subsection, we briefly review some commonly used integration methods and their errors. For illustration purpose, we consider the integral $I(f) = \int_a^b f(x)\,dx$, where f is a real bounded function over the interval $[a, b]$.

1) Midpoint rule: Under the composite midpoint rule, we approximate $I(f)$ by dividing the interval $[a, b]$ into N subintervals and employing the midpoint of each subinterval to approximate the function f. The approximation is achieved by evaluating f at the midpoints and then summing up these values weighted by the width of each subinterval. Let $H = \frac{b-a}{N}$ denote the length of each subinterval. The corresponding approximation $I_{\mathrm{m},N}(f)$ is given by

$$I_{\mathrm{m},N}(f) = H \sum_{k=0}^{N-1} f(x_k),$$

where $x_k = a + (2k+1)H/2$ for $k \in [N-1]_0$. The error is given by [15, Chapter 9.2.1]

$$I(f) - I_{\mathrm{m},N}(f) = \frac{b-a}{24} H^2 f''(\xi)$$

provided that $f \in C^2([a, b])$, i.e., the second derivative of f exists and is continuous on $[a, b]$, and where $\xi \in (a, b)$.

2) Trapezoidal rule: Under the composite trapezoidal rule, we approximate $I(f)$ by dividing the interval $[a, b]$ into N subintervals and use the endpoints of each subinterval to form a trapezoid. The approximation is then obtained by summing up the areas of these trapezoids, each weighted by the width of its corresponding subinterval. The corresponding approximation $I_{\mathrm{t},N}(f)$ is given by

$$I_{\mathrm{t},N}(f) = \frac{H}{2} \sum_{k=0}^{N-1} \left(f(x_k) + f(x_{k+1})\right),$$

where $x_k = a + kH$ for $k \in [N]_0$. The error is given by [15, Chapter 9.2.2]:

$$I(f) - I_{\mathrm{t},N}(f) = -\frac{b-a}{12} H^2 f''(\xi),$$

provided that $f \in C^2([a, b])$, i.e., the second derivative of f exists and is continuous on $[a, b]$, and where $\xi \in (a, b)$.

3) Simpson's rule: In contrast to both the composite midpoint and trapezoidal rules, Simpson's rule enhances the accuracy by approximating $I(f)$ via quadratic polynomials. This is achieved by dividing the interval into N subintervals and employing the endpoints along with the midpoints of each subinterval to construct these quadratic approximations. The composite Simpson's rule then calculates the approximation by summing up the areas under these parabolic segments, each appropriately weighted by the width of its corresponding subinterval. The corresponding approximation $I_{\mathrm{s},N}(f)$ is given by

$$\begin{aligned} I_{\mathrm{s},N}(f) = &\frac{H}{6}\Bigg(f(x_0) + 2\sum_{k=1}^{N-1} f(x_{2k}) \\ &+ 4\sum_{k=0}^{N-1} f(x_{2k+1}) + f(x_{2N})\Bigg), \end{aligned}$$

where $x_k = a + kH/2$ for $k \in [2N]_0$. The error in the composite Simpson's rule is [15, Chapter 9.2.3]

$$I(f) - I_{\mathrm{s},N}(f) = -\frac{b-a}{180} (H/2)^4 f^{(4)}(\xi),$$

provided that $f \in C^4([a, b])$, i.e., the forth derivative of f exists and is continuous on $[a, b]$, and where $\xi \in (a, b)$.

B. An example of the trapezoidal rule

In this section, we use the moments from [13, Eq. 12] as an example to explore the error from the trapezoidal rule as the evaluation parameters (step size) changes.[1] [13] considers a downlink finite cellular network where a deterministic number of transmitters N are deployed to serve the receivers. The locations of the transmitters are modeled as a uniform binomial point process in the disk $\mathbf{b}(\mathbf{o}, r_d)$. All the transmitters are active independently with probability p and transmit with unit power in each time slot. The receiver is served by the nearest transmitter, and the other $N-1$ transmitters are considered as interferers. [13] analyzes the signal-to-interference ratio for a reference receiver within the disk at $\mathbf{x}_0$, with $x_0 = \|\mathbf{x}_0\| \in [0, r_d]$. The b-th moment of the conditional success probability (with threshold θ) at $\mathbf{x}_0$ is given by

$$m_b(\theta) = \int_0^{w_p} \left(\int_r^{w_p} \left(\frac{p}{1+\theta(r/u)^\alpha} + 1 - p \right)^b f_U(u)\mathrm{d}u \right)^{N-1} f_R(r)\mathrm{d}r, \tag{7}$$

where

$$w_m = r_d - x_0, \quad w_p = r_d + x_0,$$

$$f_U(u) = \begin{cases} \frac{f_{W_1}(u)}{1-F_{W_1}(r)}, & 0 \le r \le w_m; r \le u \le w_p \\ \frac{f_{W_2}(u)}{1-F_{W_1}(r)}, & 0 \le r \le w_m; w_m \le u \le w_p \\ \frac{f_{W_2}(u)}{1-F_{W_2}(r)}, & w_m \le r \le w_p; r \le u \le w_p, \end{cases}$$

$$f_{W_1}(w) = \frac{2w}{r_d^2},$$

$$f_{W_2}(w) = \frac{2w}{\pi r_d^2} \arccos\left(\frac{w^2 + x_0^2 - r_d^2}{2x_0 w}\right)$$

$$f_R(r) = \begin{cases} f_{R_1}(r), & 0 \le r \le w_m \\ f_{R_2}(r), & w_m \le r \le w_p, \end{cases}$$

$$f_{R_1}(r) = N f_{W_1}(r)(1 - F_{W_1}(r))^{N-1},$$

$$f_{R_2}(r) = N f_{W_2}(r)(1 - F_{W_2}(r))^{N-1}.$$

$F_{W_1}(\cdot)$ and $F_{W_2}(\cdot)$ are the cdfs corresponding to $f_{W_1}(\cdot)$ and $f_{W_2}(\cdot)$.

We set $p = 1/2, r_d = 1, x_0 = r_d/2$, $\theta = 1$ and $N = 2$ and evaluate (7) using the composite trapezoidal rule and partition the integration ranges by N_{eval} evenly distributed points within the intervals (we assume F_{W_1} and F_{W_2} are accurate). Here we adopt four evaluation parameters, $N_{\text{eval}} = 11, 101, 1001$, and 2561. We denote the n-th moment under evaluation scheme N_{eval} as $m_{n,N_{\text{eval}}}$. We assume $m_{n,2561}$ is accurate enough to serve as reference. We focus on the absolute deviation (defined as $|m_{n,N_{\text{eval}}} - m_{n,2561}|$) and the relative deviation (defined as $(m_{n,N_{\text{eval}}} - m_{n,2561})/m_{n,2561}$). From the left plot of Figure 2, we observe that the absolute deviations decrease as N_{eval} increases. From the blue curve in the right plot of Figure 2, we can observe that the computation time increases drastically as N_{eval} increases, and the computational complexity is $\Theta(N_{\text{eval}}^2)$. The red curve in the same plot illustrates a linear increase in computation time with increasing N_{eval}, consistent with the fact that the moment order b does not affect the computational complexity of integral evaluation. Besides, by comparing the blue and red curves in the bottom plot of Figure 2 and combining them with the top plot, we are able to choose the suitable evaluation strategy based on our resource limitations. For instance, with approximately 4 hours of computation time, we could opt to evaluate either 2 moments with $N_{\text{eval}} = 2561$ or 5 moments with $N_{\text{eval}} \approx 1700$. As outlined in Section V, we recommend the former approach. From Table I, we can observe that for the same evaluation scheme, the relative deviation to each moment is approximately the same.

[1] As we evaluate the integrands at evenly distributed points within the defined intervals, the variations in the step sizes correspond to changes in the number of equally spaced points in those intervals. In the following, we will refer to the number of equally spaced points instead.

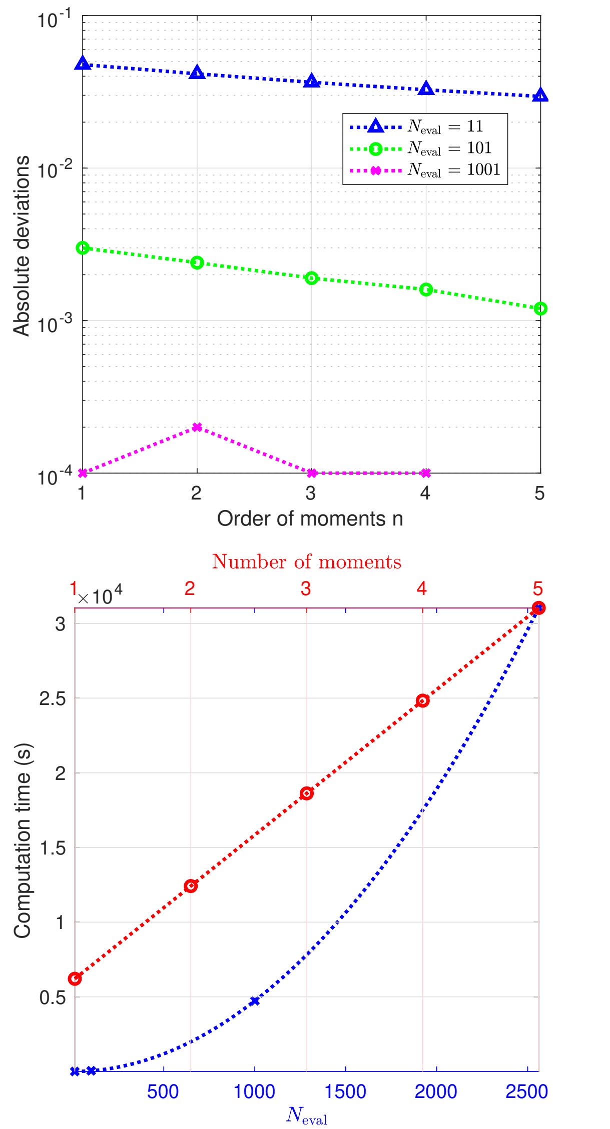

Fig. 2. The absolute deviations versus the order of moments n under different evaluation parameters (top) and computation time of 5 moments (blue) under different evaluation parameters and computation time of different number of moments (red) with $N_{\text{eval}} = 2561$ (bottom).

TABLE I
THE RELATIVE DEVIATIONS UNDER DIFFERENT EVALUATION PARAMETERS.

N_{eval}	m_1	m_2	m_3	m_4	m_5
11	-5.2%	-4.91%	-4.66%	-4.46%	-4.30%
101	-0.3%	-0.28%	-0.24%	-0.21%	-0.17%
1001	-0.01%	-0.02%	-0.01%	-0.01%	0 (exact)

C. Numerical evaluation of improper integrals: truncation

Different from the integrals of a bounded domain of integration in Section II-A, we consider improper integrals in this section. For ease of exposition, we consider integral $I(f) = \int_0^\infty f(x)\,dx$, where f is a real bounded integrable function over $[0,\infty)$.[2]

When evaluating an improper integral, there are two common methods: truncation and change of variable. These methods allow for the transformation of the improper integral into a standard integral over a finite interval, facilitating the use of numerical integration techniques suitable for such intervals. In this part, we focus only on the error associated with truncation.

When evaluating moments (obtained from improper integrals) from MDs, in most cases, the integrands are monotonic decreasing and positive. Thus, the error of the truncation is determined by the choice of integration limits, which can be easily estimated based on the decay behavior of the integrand. In general, the truncated integral is smaller than the exact one.

Next, we present an example of how the integration limit affects the accuracy of moments. [9] considers the standard downlink Poisson cellular model with base stations (BSs) forming a Poisson point process Φ, nearest-base station association, power-law path loss with path loss exponent α and Rayleigh fading. The signal-to-interference-plus-noise ratio (SINR) is considered. The n-th moment of the conditional success probability $\mathbb{P}(\mathrm{SINR} > \theta \mid \Phi)$ is given by

$$m_n(\theta) = \pi\lambda \int_0^\infty \exp\{-(A_n z + B_n z^{\alpha/2})\}\,dz, \qquad (8)$$

where $A_n = {}_2F_1(n, 1; 1-2/\alpha; \theta/(1+\theta))\pi\lambda/(1+\theta)^n$, $B_n = n\theta\sigma^2/p$, λ is the intensity of the BS point process, ${}_2F_1$ is the Gauss hypergeometric function, σ^2 is the noise power, and p is the transmit power of the BSs.

Remark 1. *If we consider the SIR instead of the SINR in* (8)*, i.e., the noise power* $\sigma^2 = 0$*, then* (8) *is simplified to [3, Theorem 2]*

$$m_n(\theta) = \frac{(1+\theta)^n}{{}_2F_1(n, 1; 1-2/\alpha; \theta/(1+\theta))}. \qquad (9)$$

In the evaluation, [9] sets $\lambda = 0.001$ per m^2, $\alpha = 5$, $\theta = 0\,\mathrm{dB}$, and $\sigma^2/p = -100\,\mathrm{dB}$. The integration limits in (8) are set to be 10, 100, 1000. As shown in Figure 3, the truncation error decreases as n increases, but the truncation error can still be significant if the integration limit is not large enough. Additionally, the right plot of Figure 3 shows that the calculated ones are smaller than the exact one.

[2]For integrands with singularities, i.e., $f(x_0)$ is undefined for some $x_0 \in [0,\infty)$, a common approach is to exclude a small neighborhood around the singularities and evaluate the limit as this neighborhood shrinks to zero.

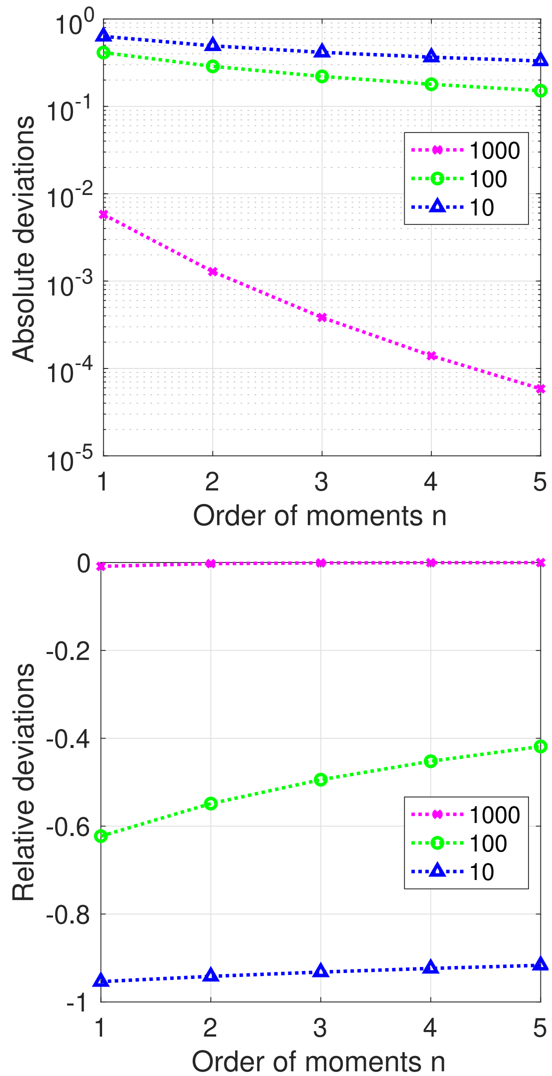

Fig. 3. The absolute deviations and relative deviations for different integration limits.

The accuracy of moments, particularly those obtained from double or triple integrals or infinite sums/integral range or approximations, is a critical concern in the reconstruction of distributions. As shown in the examples, the evaluation of integrals significantly affect the accuracy of moments. Also as shown in Section I-B, even minor variations—let alone significant perturbations—can lead to substantial alterations in the solutions to the truncated Hausdorff moment problem. This motivates us to analyze the influence of the moment inaccuracies on the reconstruction of meta distributions (MDs), and, in turn, provide guidance on optimizing the utilization of computational resources, i.e., calculating as many moments as possible vs. calculating moments as accurate as possible. In this paper, we mainly focus on the recommended reconstruction methods in [12], i.e., the beta approximation, the binomial mixture (BM) method, the Fourier-Legendre (FL) method, and the Chebyshev-Markov (CM) inequalities. In doing so, we treat the MD as a family of univariate distributions, i.e., we reconstruct the distribution of the conditional probability P_θ from its corresponding moments for multiple θ.

III. Sensitivity

A. Definition of sensitivity

To discuss the accuracy of a reconstruction method in the presence of perturbations to the moments, here we give the formal definition of the sensitivity of the moment-based reconstruction of a distribution:

Definition 1 (Sensitivity)**.** *Given a cdf F based on a moment sequence $(m_k)_{k=1}^N$, the sensitivity of F at point $x \in (0,1)$ wrt the n-th moment, where $n \in [N]$, is defined as*

$$S_{m_n}^F(x) \triangleq \lim_{\Delta m_n \to 0} \frac{\Delta F(x)/F(x)}{\Delta m_n/m_n} \tag{10}$$

$$= \frac{\mathrm{d}F}{\mathrm{d}m_n}(x) \cdot \frac{m_n}{F(x)}. \tag{11}$$

The sensitivity quantifies the change in the moment-based reconstructed distribution function to a change in a specific moment. A higher absolute sensitivity indicates that the reconstructed distribution function is more susceptible to perturbations in that particular moment. The smaller the sensitivity, the better.

Next, we calculate the sensitivity of different reconstruction methods and compare their sensitivity performance. Specifically, we focus on the beta approximation, the BM method, and the FL method.

B. Sensitivity of the beta approximation

Beta approximations are the most commonly used approximation in recovering MDs from moments [3], [4], [16]. The pdf of a beta distribution is given by

$$f_{\mathrm{Beta}}(x, \alpha, \beta) = \frac{x^{\alpha-1}(1-x)^{\beta-1}}{\mathrm{B}(\alpha, \beta)}, \tag{12}$$

where $\mathrm{Beta}(\alpha, \beta)$ is the beta function.

For the beta approximation, we use the first and second moments to match the two parameters α and β such that $\alpha = m_1(m_1 - m_2)/(m_2 - m_1^2)$ and $\beta = (1 - m_1)(m_1 - m_2)/(m_2 - m_1^2)$. For simplicity, the corresponding cdf is denoted by $F_{\mathrm{Beta}}(x)$.

Lemma 1 (Sensitivity of the beta approximation wrt m_1)**.** *The sensitivity of F_{Beta} at point x wrt m_1 is given by*

$$\begin{aligned} S_{m_1}^{F_{\mathrm{Beta}}}(x) = \Bigg(&- m_2 \frac{m_1^2 - 2m_1 + m_2}{(m_2 - m_1^2)^2} \\ &\Big(F_{\mathrm{Beta}}(x) \left(\log(x) - \psi(\alpha) + \psi(\alpha+\beta) \right) \\ &- \frac{x^{\alpha} {}_3F_2(\alpha, \alpha, 1-\beta; 1+\alpha, 1+\alpha; x)}{\mathrm{Beta}(\alpha,\beta)} \Big) \\ &+ \frac{(1+m_2)m_1^2 - 4m_1 m_2 + m_2^2 + m_2}{(m_2 - m_1^2)^2} \\ &\Big(\frac{(1-x)^{\beta} {}_3F_2(\beta, \beta, 1-\alpha; 1+\beta, 1+\beta; 1-x)}{\mathrm{Beta}(\alpha,\beta)} \\ &- \frac{\int_0^{1-x} t^{\beta-1}(1-t)^{\alpha-1}}{\mathrm{Beta}(\alpha,\beta)} \\ &(\log(1-x) - \psi(\beta) + \psi(\alpha+\beta)) \Big) \Bigg) \frac{m_1}{F_{\mathrm{Beta}(x)}}, \end{aligned}$$

where $\psi(x)$ is the digamma function.

C. Sensitivity of the BM method

A piecewise approximation of the cdf based on binomial mixtures is proposed in [17]. For any positive integer n, the approximation[3] by the BM method is defined as follows.

Definition 2 (Approximation by the BM method)**.**

$$F_{\mathrm{BM},n}(x) \triangleq \begin{cases} g_{\lfloor nx \rfloor}, & x \in (0,1], \\ 0, & x = 0, \end{cases} \tag{13}$$

where $g_l = \sum_{k=0}^{l} \sum_{i=k}^{n} \binom{n}{i}\binom{i}{k}(-1)^{i-k} m_i$, $l \in [n]_0$.

It is obvious that $g_n = 1$. We can write $\mathbf{g} \triangleq (g_l)_{l=0}^{n-1}$ as a linear transform of $\mathbf{m} \triangleq (m_l)_{l=1}^{n}$, i.e.,

$$\mathbf{g} = \mathbf{1} + \mathbf{B}\mathbf{m}, \tag{14}$$

where $\mathbf{m}$ and $\mathbf{g}$ are column vectors, $\mathbf{1}$ is the 1-vector of size n, and the transform matrix $\mathbf{B} \in \mathbb{Z}^{n \times n}$ is given by B_{kj}, $k \in [n-1]_0, j \in [n]$

$$B_{kj} \triangleq \binom{n}{j} \sum_{i=0}^{k} \binom{j}{i} (-1)^{j-i} \mathbb{1}(j \geq i), \tag{15}$$

$$= \mathbb{1}(j \geq k+1) \binom{n}{j} \sum_{i=0}^{k} \binom{j}{i} (-1)^{j-i} \mathbb{1}(j \geq i). \tag{16}$$

Compared with [8], the absolute value of each element in the proposed matrix $\mathbf{B}$ is less than or equal to its counterpart in [8]. This reduction alleviates the accuracy (digit) requirements for calculating the elements and the moments.

It is clear that $\mathbf{B}$ is an upper triangular matrix. Thus, the perturbation to m_1 only affects g_0.

Lemma 2 (Sensitivity of the BM method wrt m_1)**.** *The sensitivity of $F_{\mathrm{BM},n}$ at point x wrt m_1 is given by*

$$S_{m_1}^{F_{\mathrm{BM},n}}(x) = \begin{cases} \frac{B_{01} m_1}{g_0} \\ = -\frac{n m_1}{g_0}, \; x < 1/n \\ 0, \; x \geq 1/n. \end{cases} \tag{17}$$

Lemma 3 (Sensitivity of the BM method wrt m_k)**.** *The sensitivity of $F_{\mathrm{BM},n}$ at point x wrt m_k is given by*

$$S_{m_k}^{F_{\mathrm{BM},n}}(x) = \begin{cases} \frac{B_{(i-1)k} m_k}{g_{i-1}}, \\ x \in [\frac{i-1}{n}, \frac{i}{n}), i \in [k] \\ 0, \; x \geq k/n. \end{cases} \tag{18}$$

Lemma 2 demonstrates the robustness of the BM method to perturbations in m_1 over a wide range, and this resilience increases with the growth of n. However, due to the property of the upper triangular matrix, as shown in Lemma 3, the sensitivity of the BM method is higher for higher-order moments. This emphasizes the significance of ensuring the accuracy in the higher-order moments when applying the BM method.

Remark 2 (The sensitivity of $\mathbf{B}$)**.** *The condition number of $\mathbf{B}$ measures the relative error in $\mathbf{g}$ caused by the relative error in $\mathbf{m}$, i.e.,*

$$\frac{\|\Delta \mathbf{g}\|}{\|\mathbf{g}\|} \leq \kappa(\mathbf{B}) \frac{\|\Delta \mathbf{m}\|}{\|\mathbf{m}\|}, \tag{19}$$

[3] In this section, the term "approximation" is used when the outputs are not always solutions to the THMP.

where $\kappa(\mathbf{B})$ is the condition number of $\mathbf{B}$ and $\|\cdot\|$ is the Euclidean norm.

For $n=5$, $\kappa(\mathbf{B})=53.8$. As shown in Remark 2, the sensitivity of $\mathbf{g}$ wrt $\mathbf{m}$ is large even though that wrt the first-order moment is small.

D. Sensitivity of the FL method

For any $n\in\mathbb{N}$, the approximation obtained by the n-th partial sum of the FL expansion of the cdf F is

$$F_{\mathrm{FL},n}(x)\triangleq\sum_{l=0}^{n}c_lR_l(x),\quad x\in[0,1],\tag{20}$$

where

$$R_l(x)=\sum_{j=0}^{l}\binom{l}{j}\binom{l}{l-j}(x-1)^{l-j}x^j\tag{21}$$

is the shifted Legendre polynomial and

$$c_l=(2l+1)\sum_{k=0}^{l}(1-m_{l-k+1})\left(\frac{(-1)^k}{l-k+1}\sum_{j=0}^{l-k}\binom{l}{j}\binom{l}{l-j}\binom{l-j}{k}\right).\tag{22}$$

According to [18], we can write $\mathbf{c}=(c_l)_{l=0}^{n}$ as a linear transformation of $\hat{\mathbf{m}}=(m_k)_{k=1}^{n+1}$, i.e.,

$$\mathbf{c}=\hat{\mathbf{A}}(\mathbf{1}-\hat{\mathbf{m}}),\tag{23}$$

where $\mathbf{c}$ and $\hat{\mathbf{m}}$ are understood as column vectors, $\mathbf{1}$ is the 1-vector of size $(n+1)$, and the transform matrix $\hat{\mathbf{A}}\in\mathbb{Z}^{(n+1)\times(n+1)}$ is given by $\hat{A}_{lk}$, $k,l\in[n]_0$

$$\hat{A}_{lk}\triangleq\frac{(-1)^{(l-k)}(2l+1)}{k+1}\sum_{j=0}^{k}\binom{l}{j}\binom{l}{l-j}\binom{l-j}{l-k}\mathbb{1}(k\le l).\tag{24}$$

Since $\hat{\mathbf{A}}$ is a lower triangular matrix, the perturbation to m_1 affects all the elements in $\mathbf{c}$.

Lemma 4 (Sensitivity of the FL method wrt m_1)**.** *The sensitivity of $F_{\mathrm{FL},n}$ at point x wrt m_1 is given by*

$$S_{m_1}^{F_{\mathrm{FL},n}}(x)=\frac{-m_1\sum_{l=0}^{n}\hat{A}_{l0}R_l(x)}{F_{\mathrm{FL},n}(x)},\tag{25}$$

where $\hat{A}_{l0}=(-1)^l(2l+1)$ and $R_l(x)$ are given in (24) *and* (21)*, respectively.*

Lemma 5 (Sensitivity of the FL method wrt m_k)**.** *The sensitivity of $F_{\mathrm{FL},n}$ at point x wrt m_k is given by*

$$S_{m_k}^{F_{\mathrm{FL},n}}(x)=\frac{-m_k\sum_{l=k-1}^{n}\hat{A}_{l(k-1)}R_l(x)}{F_{\mathrm{FL},n}(x)},\tag{26}$$

where $\hat{A}_{l(k-1)}$ and $R_l(x)$ are given in (24) *and* (21)*, respectively.*

Even though Lemma 4 shows that the sensitivity of $F_{\mathrm{FL},n}$ at point x wrt m_1 is affected by multiple factors, such as

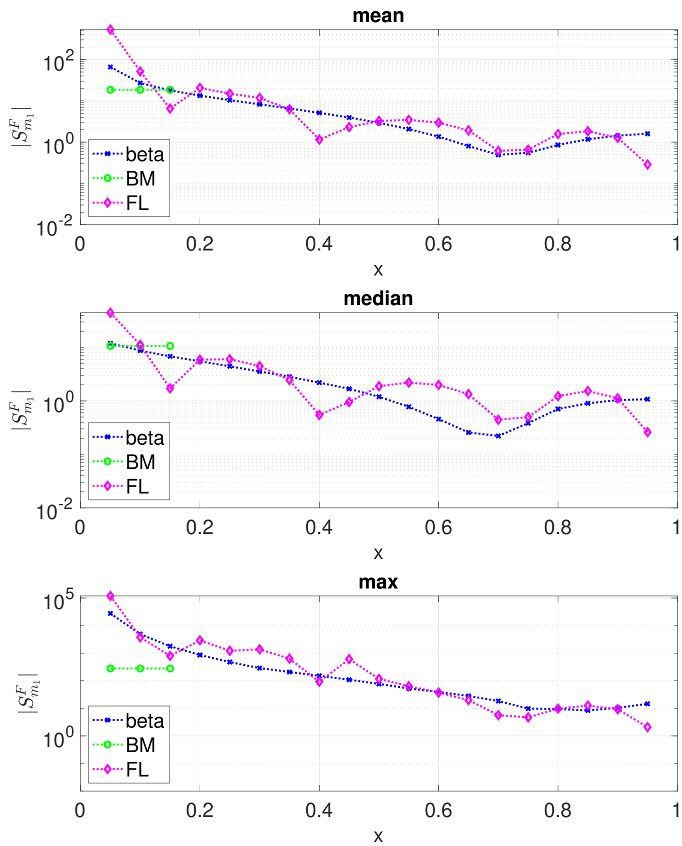

Fig. 4. The average, median, and maximum of the absolute sensitivity of each method at different x wrt m_1 for 1000 uniformly randomly generated moments of length 5 [18]. The green curves for $x\ge 1/5$ are not shown because they are zeros.

the value of $\hat{A}_{l0}$ and the value of the orthogonal polynomials $R_l(x)$, the value of $\|\hat{A}_{l0}\|=2l+1$ is not large compared to the other elements, i.e., $\|\hat{A}_{l(k-1)}\|$ in Lemma 5 for $k>1$. Besides, due to the property of the lower triangular matrix, the sensitivity of the FL method is more significantly influenced by lower-order moments. This underscores the significance of ensuring the accuracy in the lower-order moments when applying the FL method.

Remark 3 (The sensitivity of $\hat{\mathbf{A}}$)**.** *The condition number of $\hat{\mathbf{A}}$ measures the relative error in $\mathbf{c}$ caused by the relative error in $\hat{\mathbf{m}}$, i.e.,*

$$\frac{\|\Delta\mathbf{c}\|}{\|\mathbf{c}\|}\le\kappa(\hat{\mathbf{A}})\frac{\|\Delta\hat{\mathbf{m}}\|}{\|\hat{\mathbf{m}}\|},\tag{27}$$

where $\kappa(\hat{\mathbf{A}})$ is the condition number of $\hat{\mathbf{A}}$.

For $n=5$, $\kappa(\hat{\mathbf{A}})=1102$. As shown in Remark 3, the sensitivity of $\mathbf{c}$ wrt $\hat{\mathbf{m}}$ is very large, indicating that the accuracy requirement of the FL method is often very high.

Figure 4 shows the absolute sensitivity of each method at different x. The absolute sensitivity of each method is generally larger than 1 and can go up to 100 or even more at small x. This highlights the importance of the accuracy of moments when evaluating the reconstructed functions at small x. The BM method achieves zero sensitivity at $x\ge 1/5$, which is consistent with the results in Lemma 2. The absolute

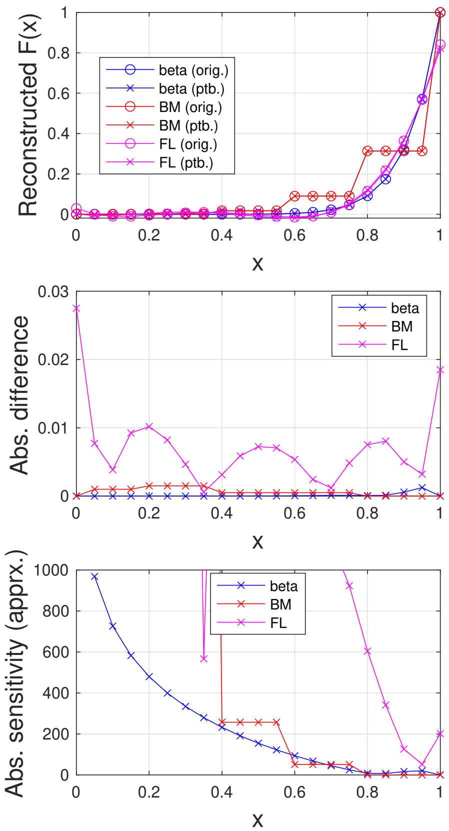

Fig. 5. The reconstructed MDs for accurate and inaccurate moments from (7) with $N_{\mathrm{eval}} = 2561$ and 1001, respectively, the corresponding absolute difference of the MDs, and the approximate absolute sensitivity wrt m_1.

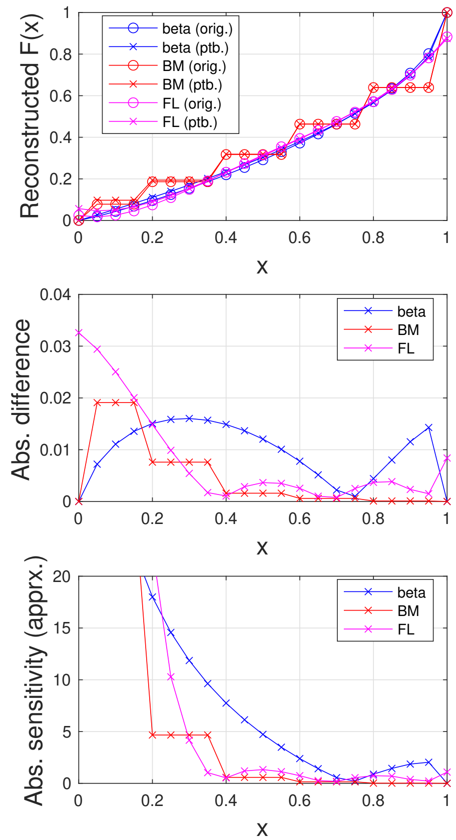

Fig. 6. The reconstructed MDs for accurate and inaccurate moments from (8) with integration limit equal to ∞ and 1000, respectively, the corresponding absolute difference of the MDs, and the approximate absolute sensitivity wrt m_1.

sensitivity of the FL method near $x = 1$ is the smallest among the three and is generally less than 1.

E. Two examples of the sensitivity of the BM and FL method

To further illustrate the implications of inaccurate moments on MD reconstructions, we explore the two types of moment sequences from Section II-B and Section II-C.

The accurate and perturbed moment sequences for Section II.B are $(0.9152,\ 0.8438,\ 0.7830,\ 0.7310,\ 0.6862)$ and $(0.9151,\ 0.8436,\ 0.7829,\ 0.7309,\ 0.6862)$, respectively. For Section II.C, the sequences are $(0.6632,\ 0.5233, 0.4458, 0.3960, 0.3608)$ and $(0.6574, 0.5220, 0.4454, 0.3958, 0.3607)$. For simplicity, we refer to these as Case 1 (Section II-B) and Case 2 (Sec. II-C) moments.

First, we verify the validity of the perturbed moment sequences, which will be discussed in more detail later in Section IV-A. Using the method mentioned in Section IV-A, we verify that the perturbed moment sequence for Case 1 is invalid, while the sequence for Case 2 is valid. Consequently, as discussed at the end of Section IV-A, the reconstructions may not preserve the properties of cdfs, such as monotonicity and boundedness within $[0, 1]$.

Figure 5 and Figure 6 display the reconstructed MDs, the absolute differences, and the approximate absolute sensitivity with respect to m_1 for both examples.

As shown in both Figure 5 and Figure 6, the "raw" reconstructions from the accurate moments using the FL method are not monotonic, which is consistent with the fact that the FL method is essentially functional approximation and does not guarantee monotonicity. Thus, as discussed in [12], we need to apply the tweaking mapping [12, Definition. 2] to obtain a sensible reconstruction. Additionally, the reconstruction from the perturbed moments of Case 1 of the BM method is not bounded in $[0, 1]$ and is not monotonic because the perturbed moment sequence is invalid.

Figure 5 and Figure 6 show that the impact on the reconstruction from the BM method is minimal (0) when $x > 0.8$. This consistency with Lemma 3 indicates that the region of $x > 0.8$ is only affected by m_5, which is accurate in the perturbed sequences for both cases. This insight is beneficial for computing the 5-th percentile, suggesting that ensuring the accuracy of certain high-order moments might suffice. Furthermore, the absolute differences in the MDs are often ten to a hundred times larger than the differences in the moments, underscoring the critical importance of moment accuracy in reconstructing MDs. The approximate absolute sensitivity of Case 1, usually greater than 100, also aligns with this finding, although it differs slightly from the results in Lemma 2 and Lemma 3 due to changes in multiple moments. Another reason why the approximate absolute sensitivity is so large in Case 1, compared with Case 2, is that the a significant portion of the reconstructions in Case 1 are close to zero and the perturbed sequence is invalid, which amplifies the impact of perturbed moments.

IV. Effect of perturbations

In Section III, we discussed the sensitivity of the reconstruction methods to the perturbations in moments, which are methods that result in approximations to the truncated Hausdorff moment problem. In this section, we will discuss the effect of perturbations to the solutions to the truncated Hausdorff moment problem, i.e., the existence of solutions and the tightest possible bounds to the solutions.

A. Validity of moment sequences

The existence of solutions to the truncated Hausdorff moment problem given a sequence is determined by the non-negativeness of the Hankel determinants of the sequence [11, Theorem. 10.1&10.2]. Here, sequences for which solutions exist are referred to as valid moment sequences, while sequences for which solutions do not exist are referred to as invalid moment sequences. In this section, we explore whether random perturbations lead to invalid moment sequences and underscore the significance of accurate moment evaluations.

Consider the case of random perturbations. Denote the initial valid moment sequence as $(m_i)_{i=1}^n$. The perturbed sequence is modeled as

$$m_i' = m_i\,(1 + V_i)\,, \quad i \in [n], \tag{28}$$

where V_i, $i \in [n]$, are i.i.d. random variables.

We use the Hankel determinants [11], [18] to verify whether a sequence is a valid moment sequence. Figure 7 shows two examples of the fraction of the invalid moment sequences subject to uniformly random perturbations. The two initial valid moment sequences are

$$\mathbf{m}_n = \left(2^{-2i}\binom{2i}{i}\right)_{i\in[n]}, \tag{29}$$

which is understood as the *center sequence*[4] because it is at the center of the moment space of length n [19], and $\mathbf{m}_n' = \left(2^{-i}\right)_{i\in[n]}$, which is understood as a *boundary sequence*[5] because it is on the boundary of the moment space of length n [19]. As the perturbation range expands or as we consider higher orders of moments, the fraction consistently rises in both cases. This observation highlights the sensitivity of the sequence to both the perturbation range and the sequence length. Remarkably, for the center sequence (29), even when the perturbation range is limited to just 1%, approximately 80% of perturbed sequences of length $n = 5$ become invalid after perturbations. In the case of the geometric sequence $\left(2^{-i}\right)_{i\in[n]}$, the percentage rises to 90% for sequences of length 3, highlighting a heightened accuracy requirement for geometric sequences (boundary sequences).

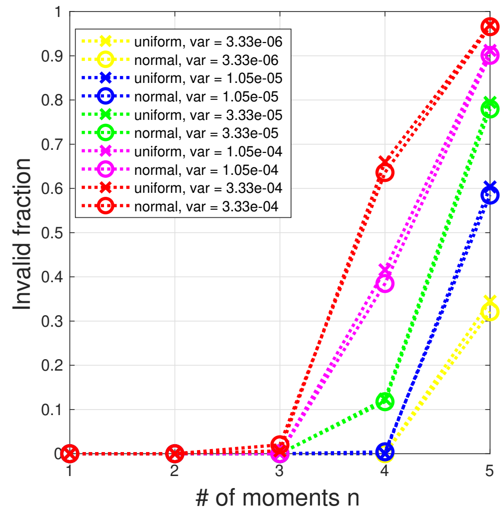

(a) Center sequence (29).

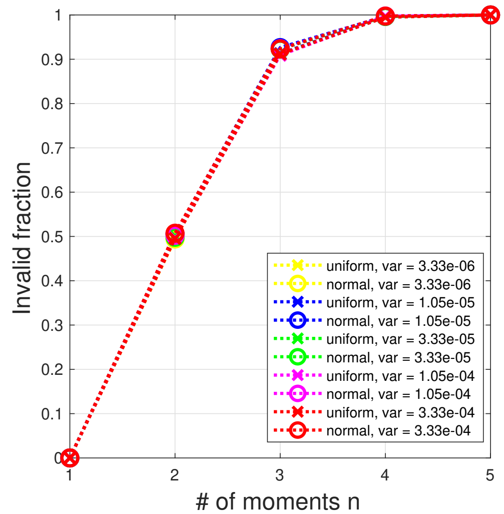

(b) $\left(2^{-i}\right)_{i\in[n]}$.

Fig. 7. The fraction of randomly perturbed sequences that are not moment sequences for the center sequence (29) and $\left(2^{-i}\right)_{i\in[n]}$ versus the highest order n based on 10000 realizations. The perturbations V_i, $i \in [n]$, are i.i.d. uniform on $[-v, v]$, where $v = 0.0032, 0.0056, 0.0100, 0.0178$, and 0.0316, corresponding to the variances in the legends. Besides, in another setting, V_i, $i \in [n]$, are i.i.d. zero-mean normal random variables with variances shown in the figure.

Intuitively, sequences near the center of the moment space are more robust compared to sequences near the boundary of the moment space. This can be explained by considering the valid range of the n-th moment given the previous $n-1$ moments. For simplicity, let us consider the case of $n = 2$. The center sequence is $(m_1, m_2) = (1/2, 3/8)$, and one of the boundary sequences is $(m_1, m_2) = (1/2, 1/4)$. For $m_1 = 1/2$, the valid range of m_2 is $[m_1^2, m_1] = [1/4, 1/2]$. The point $3/8$ from the center sequence is the middle point of this range, indicating the perturbations (in values, not in percentage) in m_2 within $[-1/8, 1/8]$ will not invalidate the moment sequence of length 2. In contrast, the point $1/4$ is at the boundary of this range, indicating that any negative perturbations invalidate the moment sequences. As for the uniform and normal distribution considered in Figure 7, this

[4] In (29), each m_i, $i \in [n]$, is obtained as the middle point of the valid range of the i-th moment determined by the previous $(i-1)$ moments, starting from $m_0 = 1$. Also, as $n \to \infty$, this sequence corresponds to the arcsine distribution with probability density function $f(x) = 1/(\pi\sqrt{x(1-x)})$.

[5] In $\mathbf{m}_n' = \left(2^{-i}\right)_{i\in[n]}$, $m_2 = 1/4$ is at the boundary of the valid range of m_2 determined by the previous moments $m_0 = 1$ and $m_1 = 1/2$, and the remaining higher-order moments are uniquely determined. Thus, $\mathbf{m}_n'$ is on the boundary of the moment space of length n [19].

corresponds to a fraction of 0.5, which is consistent with the right plot of Figure 7 at $n = 2$.

When the methods (BM, FL, and CM) are applied to invalid moment sequences, the results do not preserve the properties of cdfs, such as monotonicity and boundedness to $[0, 1]$ (see, e.g., Figures 8 to 10). These findings show the importance of prioritizing high-accuracy moment evaluations over an exhaustive assessment of a larger number of moments and the importance of determining the type of the sequences, especially those from discrete distributions which are on the boundary of the moment space.

B. The changes in the tightest possible bounds

If the validity of moment sequences is preserved after perturbations, we are interested in how the tightest possible bounds of the solutions to the truncated Hausdorff moment problem change due to the perturbations.

1) Perturbations in individual moments: In this section, we consider the changes in the tightest possible bounds with respect to perturbations in one moment, i.e., we consider the effect of perturbations in m_n for moment sequences is of length n for $n = 1$, 2, and 3. We also provide the corresponding sensitivity of the infima and suprema, respectively. The selection of m_n is based on the achievable lower and upper bounds of m_n determined by the previous $n-1$ moments, i.e.,

$$m_n^- \triangleq \min_{\lambda \in \Lambda} \{m_n(\lambda), \text{ s.t. } m_i(\lambda) = m_i, \, i \in [n-1]\}, \tag{30}$$

$$m_n^+ \triangleq \max_{\lambda \in \Lambda} \{m_n(\lambda), \text{ s.t. } m_i(\lambda) = m_i, \, i \in [n-1]\}, \tag{31}$$

where Λ is the set of probability measures on $[0, 1]$ and $m_k(\lambda) \triangleq \int_0^1 x^k \, d\lambda$. Specifically, we choose $m_n = m_n^-$, $m_n = (m_n^- + m_n^+)/2$, and $m_n = m_n^+$.

Figures 8 to 10 show the changes in the infima and suprema for different m_n under perturbations, respectively. Due to the characteristics of the provided sequences, certain perturbations lead to invalid moment sequences, resulting in corresponding bounds that exhibit non-monotonic behavior or exceed the range $[0, 1]$, as discussed at the end of Section IV-A.

We can observe that the sensitivity at the boundary, where $m_n = m_n^-$ and $m_n = m_n^+$, generally exceeds that at the middle point, where $m_n = (m_n^- + m_n^+)/2$. Also, the changes in the infima and suprema are more significant at the boundary. To quantify this relationship between sensitivity and proximity to the boundary, we propose the following *robustness metric*.

Definition 3 (Robustness metric)**.** *For a given sequence $\mathbf{m}_n = (m_k)_{k \in [n]}$, the robustness metric is defined as*

$$\mathrm{RM}(\mathbf{m}_n) = \min_{k \in [n]} \min \left(\frac{|m_k - m_k^-|}{|m_k^+ - m_k^-|}, \frac{|m_k - m_k^+|}{|m_k^+ - m_k^-|} \right), \tag{32}$$

where m_k^- and m_k^+ are given in (30) *and* (31)*, respectively.*

It is obvious that $\mathrm{RM}(\mathbf{m}_n) \in [0, 0.5]$.

Lemma 6 (Distribution of the robustness metric)**.** *For uniformly distributed random moment sequences of length n, the cdf $F_{\mathrm{RM}(\mathbf{m}_n)}$ of $\mathrm{RM}(\mathbf{m}_n)$ is given by*

$$F_{\mathrm{RM}(\mathbf{m}_n)}(x) = 1 - \prod_{k \in [n]} \left(1 - 2F_{\mathrm{Beta}}(x, k, k)\right), \tag{33}$$

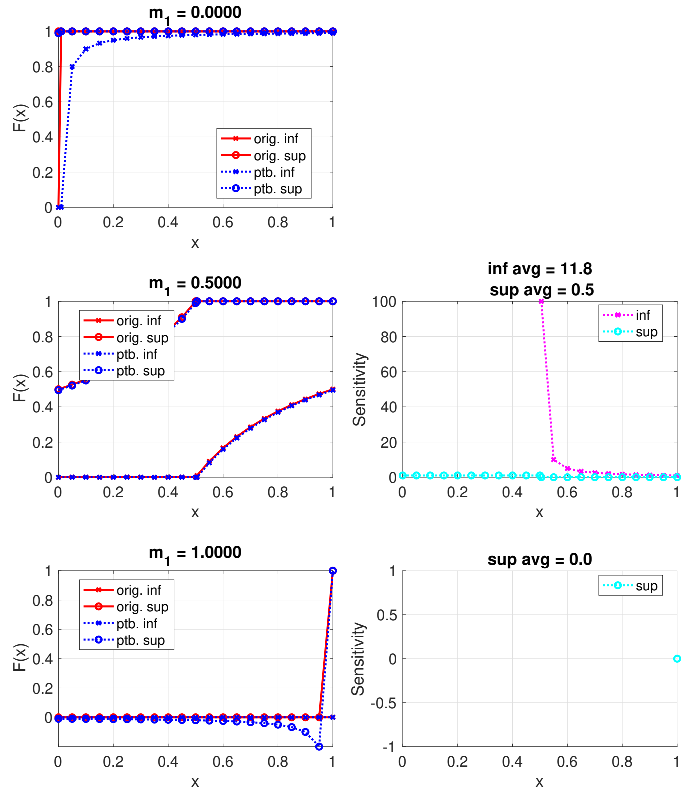

Fig. 8. The infima and suprema at $n = 1$ and corresponding sensitivity at different x. The perturbed $m_1' = m_1(1 + 0.01)$ for $m_1 > 0$, and $m_1' = m_1 + 0.01$ for $m_1 = 0$. The sensitivity is shown at points where $F(x) > 0$ and $m_1 > 0$. For $m_1 = 0$, the plot is left blank. The average of the sensitivity is calculated based on the shown points.

where $F_{\mathrm{Beta}}(x, k, k)$ is the corresponding cdf of the beta distribution whose pdf is given in (12)*.*

Proof. By [19, Theorem 1.3], for uniformly distributed random moment sequences of length n, the canonical coordinates p_k, $k \in [n]$, defined as

$$p_k = \frac{m_k - m_k^-}{m_k^+ - m_k^-} \tag{34}$$

are independently distributed with the same beta distribution $\mathrm{Beta}(n-k+1, n-k+1)$. With p_k, the robustness metric of $\mathbf{m}_n$ can be expressed as

$$\mathrm{RM}(\mathbf{m}_n) = \min_{k \in [n]} \min(p_k, 1 - p_k). \tag{35}$$

Therefore, by the independence of p_k, $k \in [n]$, and the property of the minimum function in the robustness metric,

$$\begin{aligned} &\bar{F}_{\mathrm{RM}(\mathbf{m}_n)}(x) \\ &= \prod_{k \in [n]} (p_k \geq x, 1 - p_k \geq x) \qquad (36) \\ &= \prod_{k \in [n]} (1 - 2F_{\mathrm{Beta}}(x, n-k+1, n-k+1)) \qquad (37) \\ &= \prod_{k \in [n]} (1 - 2F_{\mathrm{Beta}}(x, k, k)) \, . \qquad (38) \end{aligned}$$

$\square$

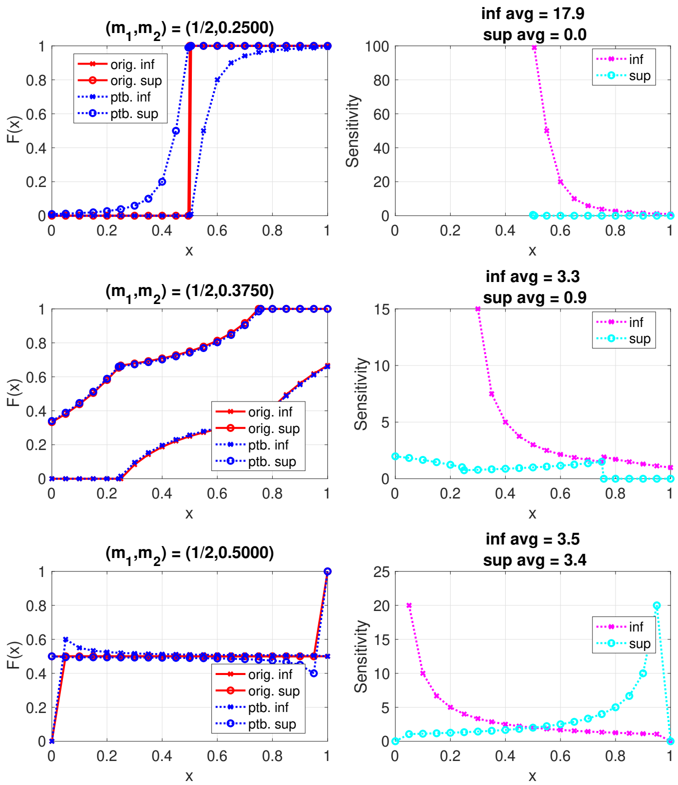

Fig. 9. The infima and suprema at $n = 2$ for different m_2 (given $m_1 = 1/2$) and corresponding sensitivity at different x. The perturbed $m_2' = m_2(1 + 0.01)$. The sensitivity is shown at points where $F(x) > 0$. The average of the sensitivity is calculated based on the shown points.

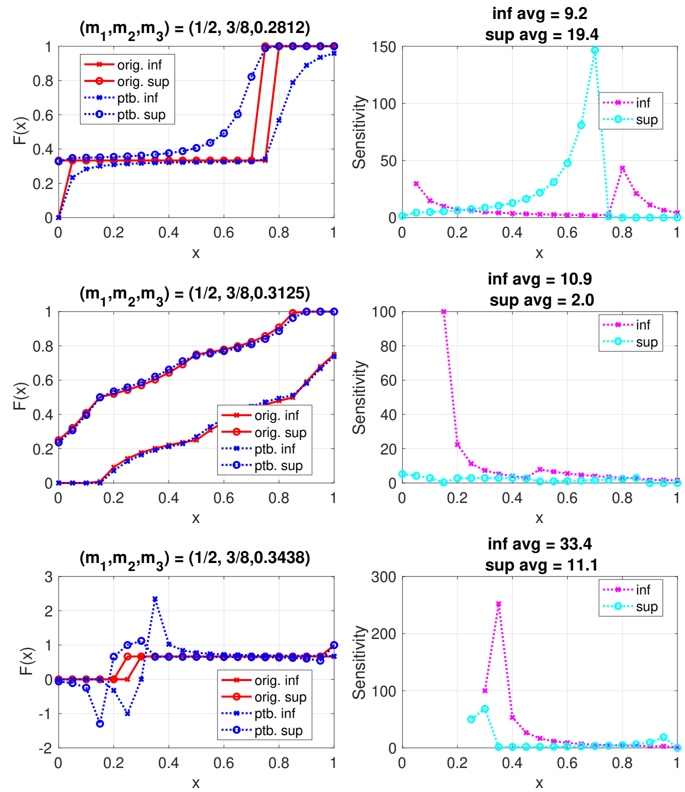

Fig. 10. The infima and suprema at $n = 3$ for different m_3 (given $(m_1, m_2) = (1/2, 3/8)$) and corresponding sensitivity at different x. The perturbed $m_3' = m_3(1 + 0.01)$. The sensitivity is shown at points where $F(x) > 0$. The average of the sensitivity is calculated based on the shown points.

As shown in Lemma 6 and Figure 11, the robustness metric is concentrated more around 0 compared to 0.5, and the longer the sequence is, the more skewed it is towards 0. Intuitively, for the robustness metric to approach 0.5, all moments must cluster tightly near the center. Conversely, for the metric to approach 0, only one moment needs to approach the boundary, which is a much less stringent condition. Also, as shown in Figure 11, about 10% of the uniformly distributed moment sequences have a robustness metric smaller than 0.05. The situation is even worse for the actual moment sequences. As shown in Figure 12, about 40% of the sequences have the robustness metrics smaller than 0.05.

Figure 13 and Figure 14 show the sensitivity of the beta approximation and the BM and FL method for randomly generated sequences with different values of the robustness metric. Comparing the two, we observe that the median of the sensitivity of the beta approximation stays almost the same, while the mean and maximum value of the sensitivity of the beta approximation are significantly higher for sequences with robustness metrics smaller than 0.05, suggesting the presence of outliers when the sequence is near the boundary. However, whether the sequence is close to the boundary or not has little impact on the sensitivity of the BM and FL method. Also, from Figure 4 and Figure 14, we observe that the sensitivity of the methods for sequences with robustness metrics larger than 0.45 is of the same magnitude as the sensitivity of the methods for uniformly randomly generated moment sequences.

The closer $\mathrm{RM}(\mathbf{m}_n)$ is to zero, the more "dangerous" we

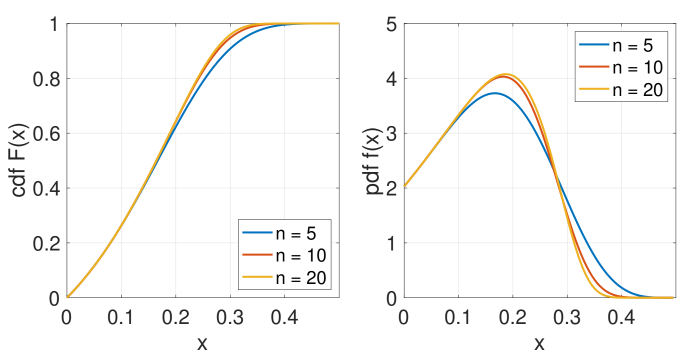

Fig. 11. The cdf (left) and pdf (right) of the robustness metric for uniformly randomly generated moment sequences of length $5, 10$, and 20.

consider the sequence to be. For example, $\mathrm{RM}(\mathbf{m}_n) \le 0.05$ can be a red flag. The robustness metric serves as an indicator of how careful we need to be when calculating moments and how sensitive the reconstructed function could be.

2) Perturbations across all moments: Here, we assume the perturbations, i.e., $(m_i' - m_i)/m_i$, are the same for each

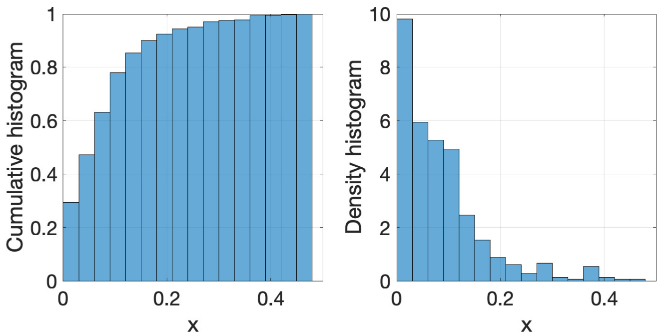

Fig. 12. The cumulative and density histogram of the robustness metric for 500 randomly generated moment sequences of length 5 given in (8), where $\lambda \sim \text{Unif}(5 \times 10^{-5}, 10^{-3})$, $\alpha \sim \text{Unif}(2, 4)$, $\theta \sim \text{Unif}(0.1, 40)$, and $\sigma^2/p \sim \text{Unif}(10^{-14}, 10^{-10})$.

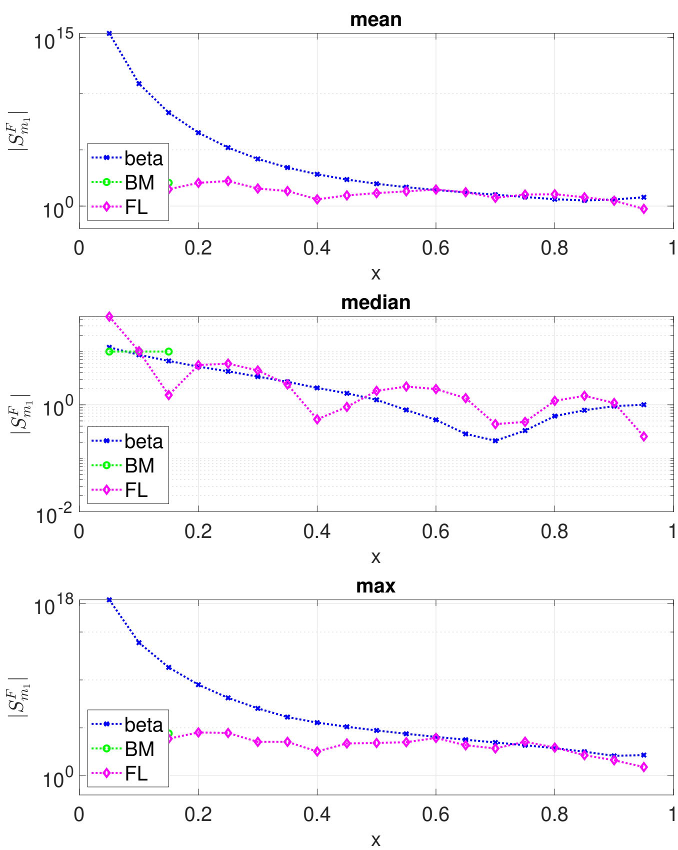

Fig. 13. The average, median, and maximum of the absolute sensitivity of each method at different x wrt m_1 for 1000 randomly generated moments of length 5 with $\text{RM}(\mathbf{m}_5) \leq 0.05$. The green curves for $x \geq 1/5$ are not shown because they are zeros.

$i \in [n]$.[6] As discussed in Section II-A and Section II-C, it is evident that the perturbations are less likely to be independent across each moment, which justifies the assumption of

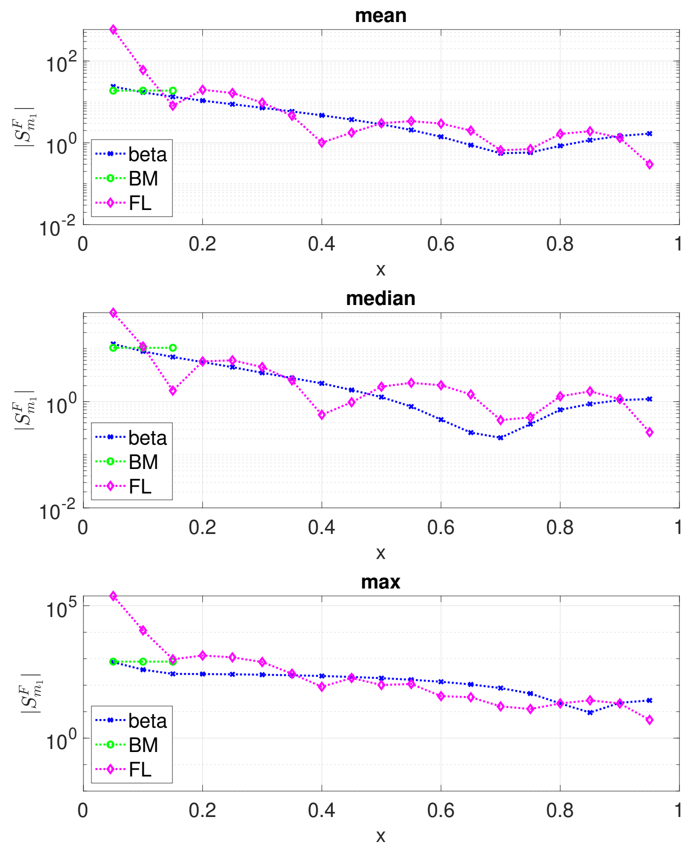

Fig. 14. The average, median, and maximum of the absolute sensitivity of each method at different x wrt m_1 for 1000 randomly generated moments of length 5 with $\text{RM}(\mathbf{m}_5) \geq 0.45$. The green curves for $x \geq 1/5$ are not shown because they are zeros.

correlation. For ease of exposition, the perturbed sequence is modeled as

$$m_i' = m_i(1 + V), \quad i \in [n], \tag{39}$$

where $V \in [-0.05, 0.05]$ is a uniform random variable.[7]

Figure 15 gives an example how the infima and suprema from the CM inequalities change due to the perturbations to each element in the moment sequence $(1/2, 3/8, 5/16, 35/128, 63/256)$, which is exactly the center sequence in (29) at $n = 5$. From Figure 15, we observe that the infima and suprema after negative perturbations are greater than the initial ones while the infima and suprema after positive perturbations are smaller than the initial ones. This observation for the negative perturbations can be easily explained from Footnote 6 and the fact that $F(x) \leq rF(x) + (1 - r)$ for all $0 \leq r \leq 1$. For the positive perturbations, it cannot be easily proved, but we can illustrate it by Example 2. Suppose the initial moment sequence is (m_1) and the perturbed one is $(rm_1), 1 < r \leq 1/m_1$. For (m_1), the infima are $1 - m_1/x$ within $x \in (m_1, 1]$, while for (rm_1), the infima are $1 - rm_1/x$ within $x \in (rm_1, 1]$. Since $r > 1$, $m_1 < rm_1$ and $1 - rm_1/x < 1 - m_1/x$. Combined with the fact that the infima stay 0 within $x \in [0, m_1]$ and $x \in [0, rm_1]$, it is clear

[6] As shown in Section IV-A, if the perturbations are not the same for each element, it is very likely that the perturbed sequence of length 5 does not form a valid moment sequence, even if the perturbations are very small, e.g., less than 2.5%. Conversely, if the perturbations are uniform and negative, it can be easily shown that the downsized version of a solution to the original moment sequence is a solution to the perturbed sequence, i.e., a pdf $rf(x) + (1 - r)\delta(x)$ corresponds to the moment sequence $r\mathbf{m}$, $r \in (0, 1)$, if a pdf f corresponds to $\mathbf{m}$.

[7] For the purpose of exploring the effect of perturbations on the achievable bounds, it would be justified to model them as distributions with bounded support.

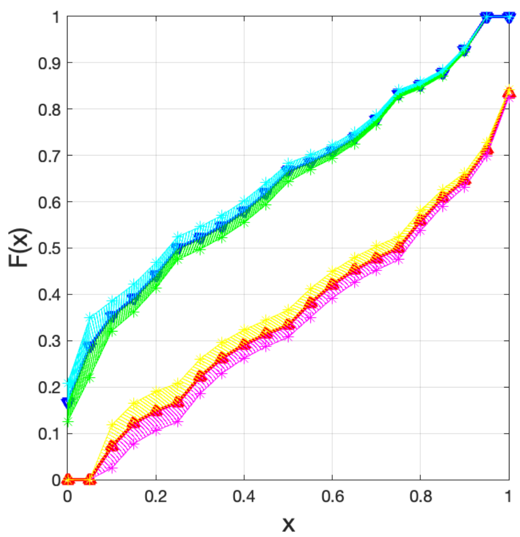

Fig. 15. The infima and suprema from the CM inequalities for 2000 moment sequences $(m_1, m_2, .., m_5)$ given an initial moment sequence $(1/2, 3/8, 5/16, 35/128, 63/256)$ with a random perturbation to each element no larger than $\pm 5\%$. The perturbation to each element are the same. The infima and suprema for positive perturbations are in magenta and green, respectively. The infima and suprema for negative perturbations are in yellow and cyan, respectively. The infima and suprema obtained at the perturbation limit ($\pm 5\%$) are marked by $*$. The infima and suprema from the CM inequalities for the moment sequence $(1/2, 3/8, 5/16, 35/128, 63/256)$ are given in $\triangle$ and $\bigtriangledown$, respectively.

that the infima after positive perturbations are smaller than the initial ones. Simulations in Figure 15 also shows that the greatest upper bound is achieved when the perturbation is at the negative limit, which is -5% in this case. This follows from the fact that $rF(x) + (1 - r) \le r'F(x) + (1 - r')$ for $0 \le r' < r < 1$.

Example 2 $(n = 1)$**.** *For $n = 1$, the infima and suprema are*

$$\inf_{F \in \mathcal{F}_1} F(x) = \begin{cases} 0,\ 0 \le x \le m_1, \\ 1 - \frac{m_1}{x},\ m_1 < x \le 1, \end{cases} \tag{40}$$

$$\sup_{F \in \mathcal{F}_1} F(x) = \begin{cases} \frac{1-m_1}{1-x},\ 0 \le x \le m_1, \\ 1,\ m_1 < x \le 1. \end{cases} \tag{41}$$

The infima are equivalent to Markov's inequality.

We may also use Example 2 and Example 1 to explain why the suprema are less sensitive to perturbations when x is very close to 1 and why the infima are less sensitive to perturbations when x is close to 0. Consider Example 1 with $n = 2$. Let the perturbed moments to be (km_1, km_2). The range $(\frac{m_2}{m_1}, 1]$ does not change under the perturbed moments for both the infima and suprema. In this range, the suprema are always 1. Similarly, on the interval $[0, \frac{m_1 - m_2}{1 - m_1}]$, the infima are always 0, but the range changes as k changes.

From Figure 15, we can also observe that symmetric perturbations do not result in symmetric changes in the bounds.

V. Recipe for Moment Computation and Reconstruction Method Selection

In this section, we present the procedure of calculating moments and the suggested method based on the known information of the moment sequences.

For a given moment expression, we initially compute the first two moments with a predetermined level of accuracy.[8] Subsequently, we use the Hankel determinants to assess the validity of the moment sequence, calculate the robustness metric of the current moment sequence, and make necessary adjustments. Specifically, if the moment sequence is valid, we proceed to calculate the robustness metric. If the robustness metric is greater than 0.05, we continue to calculate the next moment using the current accuracy setting; otherwise, we set a flag or perform additional checks or corrections to ensure the sequence's proximity to the boundary is due to the underlying distribution and not inaccurate evaluation. If the moment sequence is found to be invalid, we escalate the accuracy setting and recalculate the current moments. This iterative process continues until the resource limit is reached. For a pseudo code of this procedure, refer to Algorithm 1.

Algorithm 1 Algorithm for calculating a moment sequence for the MD reconstruction

Input: The moment expression $m_n = M(n)$, the predetermined level of accuracy, and resource limit.
Output: The calculated sequence $(m_k)_{k=1}^n$.

Calculate m_1 and m_2 based on the predetermined level of accuracy and set $n = 2$.
while resource limit is not reached **do**
  Check the validity of the calculated sequence $(m_k)_{k=1}^n$ using the non-negativeness of the Hankel determinants [18].
  if the sequence $(m_k)_{k=1}^n$ is a valid moment sequence **then**
    Calculate the robustness metric $\mathrm{RM}(\mathbf{m}_n)$.
    if $\mathrm{RM}(\mathbf{m}_n) > 0.05$ **then**
      Calculate m_{n+1} based on the current accuracy setting and set $n = n + 1$.
    else
      Set a flag or perform additional checks or corrections to ensure the sequence's proximity to the boundary is due to the underlying distribution and not inaccurate evaluation.
    end if
  else
    Increase the accuracy setting and recalculate $(m_k)_{k=1}^n$ based on the current accuracy setting.
  end if
end while

Next, based on the nature of the evaluation method and moment expressions, only two moments are available, the beta approximation is preferred. Otherwise, if the lower-order

[8] Here we assume the computational resources suffice to calculate two moments under the predetermined level of accuracy. Otherwise, we decrease the predetermined level of accuracy to satisfy the computational resource limit.

moments are known to be accurate, we recommend using the FL method, and if the accuracy of moments are unknown, we suggest using the BM method. Note that when the beta approximation is chosen and the robustness metric is smaller than 0.05, it is suggested to perform additional checks or corrections to ensure the sequence's proximity to the boundary is due to the underlying distribution and not due to inaccurate evaluation.

VI. Conclusion

Numerically computed moments deviate from the exact ones. This paper addresses a critical issue encountered during the reconstruction of MDs from moments, where the calculated moments are subject to perturbations. We explore the common sources of perturbations in the evaluation of moments, analyze the sensitivity of reconstruction methods to perturbations, and discuss their impact on MD reconstructions. Additionally, we provide guidelines for effectively computing and utilizing moments in MD reconstructions. They underscore the importance of prioritizing the accuracy of moments over the quantity of calculated moments during the computation process.

References

[1] "Minimum requirements related to technical performance for IMT-2020 radio interface(s)," https://www.itu.int/dms_pub/itu-r/opb/rep/R-REP-M.2410-2017-PDF-E.pdf, accessed: 2022-05-31.

[2] "11ax Evaluation Methodology," https://mentor.ieee.org/802.11/dcn/14/11-14-0571-12-00ax-evaluation-methodology.docx, accessed: 2022-04-13.

[3] M. Haenggi, "The Meta Distribution of the SIR in Poisson Bipolar and Cellular Networks," *IEEE Transactions on Wireless Communications*, vol. 15, no. 4, pp. 2577–2589, 2016.

[4] Y. Wang, Q. Cui, M. Haenggi, and Z. Tan, "On the SIR Meta Distribution for Poisson Networks With Interference Cancellation," *IEEE Wireless Communications Letters*, vol. 7, no. 1, pp. 26–29, 2018.

[5] Y. Wang, M. Haenggi, and Z. Tan, "SIR Meta Distribution of K-Tier Downlink Heterogeneous Cellular Networks With Cell Range Expansion," *IEEE Transactions on Communications*, vol. 67, no. 4, pp. 3069–3081, 2019.

[6] K. Feng and M. Haenggi, "Separability, Asymptotics, and Applications of the SIR Meta Distribution in Cellular Networks," *IEEE Transactions on Wireless Communications*, vol. 19, no. 7, pp. 4806–4816, 2020.

[7] J. P. Jeyaraj, M. Haenggi, A. H. Sakr, and H. Lu, "The Transdimensional Poisson Process for Vehicular Network Analysis," *IEEE Transactions on Wireless Communications*, vol. 20, no. 12, pp. 8023–8038, 2021.

[8] M. Haenggi, "Efficient Calculation of Meta Distributions and the Performance of User Percentiles," *IEEE Wireless Communications Letters*, vol. 7, no. 6, pp. 982–985, 2018.

[9] S. Guruacharya and E. Hossain, "Approximation of Meta Distribution and Its Moments for Poisson Cellular Networks," *IEEE Wireless Communications Letters*, vol. 7, no. 6, pp. 1074–1077, 2018.

[10] J. Shohat and J. Tamarkin, *The Problem of Moments*, ser. Mathematical surveys and monographs. American Mathematical Society, 1950.

[11] K. Schmüdgen, *The moment problem*. Berlin: Springer, 2017.

[12] X. Wang and M. Haenggi, "Fast Hausdorff Moment Transforms for Meta Distributions in Wireless Networks," *IEEE Transactions on Wireless Communications*, vol. 23, no. 4, pp. 2607–2621, 2024.

[13] N. Kouzayha, H. Elsawy, H. Dahrouj, and T. Y. Al-Naffouri, "Meta Distribution of Downlink SIR for Binomial Point Processes," *IEEE Wireless Communications Letters*, vol. 10, no. 7, pp. 1557–1561, 2021.

[14] A. Markoff, "Démonstration de certaines inégalités de M. Tchébychef," *Mathematische Annalen*, vol. 24, no. 2, pp. 172–180, 1884.

[15] A. Quarteroni, R. Sacco, and F. Saleri, *Numerical mathematics*. Berlin: Springer, 2007, vol. 37.

[16] X. Tang, X. Xu, and M. Haenggi, "Meta Distribution of the SIR in Moving Networks," *IEEE Transactions on Communications*, vol. 68, no. 6, pp. 3614–3626, 2020.

[17] R. Mnatsakanov and F. Ruymgaart, "Some properties of moment-empirical cdf's with application to some inverse estimation problems," *Mathematical Methods of Statistics*, vol. 12, no. 4, pp. 478–495, 2003.

[18] X. Wang and M. Haenggi, "Hausdorff Moment Transforms and Their Performance," 2022. [Online]. Available: https://arxiv.org/abs/2212.12622

[19] F.-C. Chang, J. Kemperman, and W. Studden, "A Normal Limit Theorem for Moment Sequences," *The Annals of Probability*, vol. 21, no. 3, pp. 1295–1309, 1993.

Xinyun Wang (S'23) received her B.S. degree in Information Engineering from the Shanghai Jiao Tong University, China, in 2019. She received her Ph.D. degree in Electrical Engineering at the University of Notre Dame, Notre Dame, IN, USA, in 2024. Her scientific interests include wireless communications and networks and stochastic models.

Martin Haenggi (S'95-M'99-SM'04-F'14) received the Dipl.-Ing. (M.Sc.) and Dr.sc.techn. (Ph.D.) degrees in electrical engineering from the Swiss Federal Institute of Technology in Zurich (ETHZ) in 1995 and 1999, respectively. Currently he is the Freimann Professor of Electrical Engineering and a Concurrent Professor of Applied and Computational Mathematics and Statistics at the University of Notre Dame, Indiana, USA. In 2007-2008, he was a Visiting Professor at the University of California at San Diego, in 2014-2015 he was an Invited Professor at EPFL, Switzerland, and in 2021-2022 he was a Guest Professor at ETHZ. He is a co-author of the monographs "Interference in Large Wireless Networks" (NOW Publishers, 2009) and "Stochastic Geometry Analysis of Cellular Networks" (Cambridge University Press, 2018) and the author of the textbook "Stochastic Geometry for Wireless Networks" (Cambridge, 2012) and the blog stogblog.net. His scientific interests lie in networking and wireless communications, with an emphasis on cellular, amorphous, ad hoc (including D2D and M2M), cognitive, vehicular, and wirelessly powered networks. He served as an Associate Editor for the Elsevier Journal of Ad Hoc Networks, the IEEE Transactions on Mobile Computing (TMC), the ACM Transactions on Sensor Networks, as a Guest Editor for the IEEE Journal on Selected Areas in Communications, the IEEE Transactions on Vehicular Technology, and the EURASIP Journal on Wireless Communications and Networking, as a Steering Committee member of the TMC, and as the Chair of the Executive Editorial Committee of the IEEE Transactions on Wireless Communications (TWC). From 2017 to 2018, he was the Editor-in-Chief of the TWC. For both his M.Sc. and Ph.D. theses, he was awarded the ETH medal. He also received a CAREER award from the U.S. National Science Foundation in 2005 and three paper awards from the IEEE Communications Society, the 2010 Best Tutorial Paper award, the 2017 Stephen O. Rice Prize paper award, and the 2017 Best Survey paper award, and he is a Clarivate Analytics Highly Cited Researcher.